HiSST: 3rd International Conference on
High-Speed Vehicle Science Technology
14 -19 April 2024, Busan, Korea

Knowledge Discovery on Cavity-Based Scramjet Combustor Design via Stochastic-Surrogate-Assisted Multi-Objective Optimization

Chihiro Fujio[1], Sasi Kiran Palateerdham[2], Lakshmi Narayana Phaneendra Peri[3], Hideaki Ogawa[4], and Antonella Ingenito[5]

Abstract

Scramjet engines are a promising propulsion system for hypersonic flights in high-speed point-to-point transportation and space transportation. Although the scramjet technology has reached the level of successful in-flight operation, there still remain various challenges in scramjet combustor design, including significant costs for numerical simulations. While multi-objective optimization is one of the most effective approaches for design exploration, substantial costs for function evaluations render the combustor design optimization unrealistic. The present study aims to enable efficient yet high-fidelity design exploration of scramjet combustors. As a preliminary study, this paper presents the results of data mining and model-based optimization based on a relatively small dataset of scramjet combustor flowfields from numerical simulations. Key design factors have been revealed including (1) the desirable flow structure in the vicinity of the cavity and the secondary injector and (2) influential design parameters on mixing efficiency, combustion efficiency, pressure rise, and thrust. Also discussed is provided on a surrogate modeling approach that is possible with a relatively small number of reacting flowfield simulations.

Keywords: *scramjet engine*, *supersonic combustion*, *multi-objective optimization*, *machine learning*

1. Introduction

Supersonic combustion ramjet (scramjet) engines are hypersonic airbreathing engines expected to play an important role in future high-speed transportation. In particular, atmospheric flights in space transportation are situations that take advantage of scramjet engines, such as their acceleration capability to high Mach numbers and their airplane-like operation, which enables the reuse of vehicles, thus facilitating frequent and economical transportation. The research and development of scramjet engines have continued for over 70 years, reaching the level of successful in-flight demonstration of scramjet-powered flights. A remarkable milestone was achieved in the HyShot-2 program, in which the world's first in-flight supersonic combustion was demonstrated [1], followed by several successes of flight experiments, including the Hyper-X program, which marked the world's fastest jet propulsion by scramjet [2] and the Boeing X-51 flight test, which recorded the longest duration of scramjet-powered flights [3]. While several flight experiments of scramjet vehicles have concluded successfully, further enhancement of scramjet performance is needed to put scramjet engines into practice. One of the

[1] *Department of Aeronautics and Astronautics, Kyushu University, 744 Motooka Nishi-ku, Fukuoka 819-0385, Japan, fujio.chihiro.354@s.kyushu-u.ac.jp*
[2] *School of Aerospace Engineering, La Sapienza University of Rome, Via Slaria 851, 00138, Roma RM, Italy, sasikiran.palateerdham@uniroma1.it*
[3] *School of Aerospace Engineering, La Sapienza University of Rome, Via Slaria 851, 00138, Roma RM, Italy, phanindra.p123@gmail.com*
[4] *Department of Aeronautics and Astronautics, Kyushu University, 744 Motooka Nishi-ku, Fukuoka 819-0385, Japan, hideaki.ogawa@aero.kyushu-u.ac.jp*
[5] *School of Aerospace Engineering, La Sapienza University of Rome, Via Slaria 851, 00138, Roma RM, Italy, antonella.ingenito@uniroma1.it*

biggest knowledge gaps is the design strategy of scramjet engines, particularly their combustors, which requires careful consideration of complicated aerothermodynamics as well as chemical reactions.

Among various design approaches for scramjet engines, utilizing optimization algorithms for design exploration shows promise. Population-based multi-objective design optimization (MDO) approaches, such as evolutionary algorithms, are widely recognized as powerful tools for not only design exploration but also for extracting key design factors and developing design strategies. Preceding studies reported MDO studies of scramjet components including intakes [4], fuel injectors [5], and nozzles [6]. However, there are few studies that have conducted MDO investigations via population-based approaches for scramjet combustors due to significant computational costs. Kumar *et al*. reported MDO of a scramjet combustor with three instream strut injectors using complex-box algorithms and the Kriging method, which replaced CFD simulations with a regression function [7]. They conducted 64 CFD simulations for design exploration, which may be insufficient to build accurate surrogate models. Additionally, the single-step chemical reaction mechanism employed in the study is known to be erroneous due to incorrect ignition delay [8]. Ogawa *et al*. conducted an MDO study for an axisymmetric scramjet intake and combustor assuming an inviscid regime and hydrogen-air premixed inflow [9]. While the study performed at least 100 CFD simulations, it did not achieve adequate design of the axisymmetric intake and combustor. Even with recent advancements in computational capabilities, MDO of scramjet combustors remains a challenging task due to the computational cost of CFD simulations. Mitigating computational costs for design exploration is crucial to enable more realistic and detailed exploration of scramjet combustor designs and to establish effective design strategies.

To reduce the cost of CFD simulations, machine learning techniques, including deep learning, are often employed for data-driven predictive modeling. All of the MDO studies mentioned above [4-7,9] utilize various surrogate models to predict objective and constraint function values based on the decision variables. While such machine learning techniques offer a significant reduction in computational cost once accurate modeling is achieved, generating a sufficiently large dataset requires substantial computational resources, particularly in the case of combustor simulations. Therefore, it is important to develop surrogate modeling techniques or new types of surrogate models that require a relatively small amount of training data.

The present study aims to conduct a multi-objective design optimization study to gain insights into scramjet combustor design and establish its design strategy by developing a new data-efficient surrogate modeling technique. This paper reports preliminary investigations, including dataset generation, data mining, surrogate modeling, and model-based multi-objective design optimization. The study focuses on a two-dimensional cavity-based scramjet combustor designed according to the HIFiRE-2 program [10], with 100 geometries examined using CFD simulations. Suitable design features are discussed based on the CFD results, and the results of MDO are used to validate the findings.

2. Methodology

2.1. Configuration

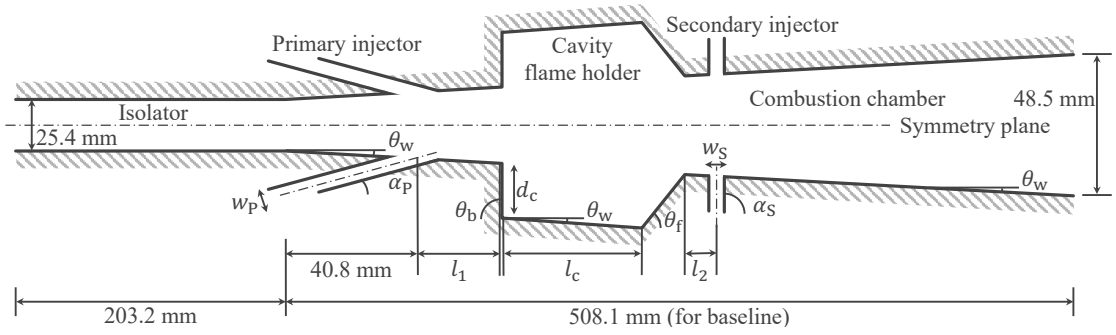

Fig. 1 Parameterization of cavity-based scramjet combustor

The present study considers the design of a two-dimensional scramjet combustor with 4 slot injectors and cavity flame holders based on the design employed for the HIFiRE-2 program [10]. The vertically symmetrical geometry of the scramjet combustor is controlled by 11 design variables which are schematically shown in Fig. 1. The wall of the combustion chamber has a constant diverging angle θ_W

to avoid thermal choke, generating thrust. The cavities are installed to stabilize and help maintaining supersonic combustion and their shapes are represented by the depth d_c, length l_c, inclination angles of backward and forward facing steps θ_b and θ_f, and the location is determined by the distance from the center of the primary injector l_1. Fuel injection is controlled by the angles of injectors α_P and α_S, widths of injectors w_P and w_S, distance between the end of the cavity and the secondary injector l_2, as well as the equivalence ratios of primary injectors Φ_1, while the total equivalence ratio Φ of 1 is maintained to facilitate the comparison among various designs and the baseline design. The values of design variables of the baseline geometry is determined based on the original HIFiRE-2 combustor.

The present study employs hydrogen as the fuel due to its wide flammability limits and minimum ignition energy, whereas the original study considered JP-7, which is a mixture of 36 % methane and 64 % ethylene. The operating condition and isolator inflow condition are also determined based on Ref. [10], as summarized in Table 1. The injection pressure for each injector is determined based on the equivalent ratio and slot width of each injector.

Table 1 Inflow and injection conditions

Inflow	Static pressure	Static temperature	Mach number	Gas composition in mole fraction
Isolator	40.3 kPa	736.2 K	3.46	O_2 (21 %), N_2 (79 %)
Primary injector	-	293.3 K	1	H_2 (100 %)
Secondary injector	-	301.1 K	1	H_2 (100 %)

2.2. Computational Fluid Dynamics (CFD)

The present study employs the state-of-art commercial solver CFD++, which is developed by Metacomp Technologies [11] and has been employed by Australian hypersonics network for scramjet research due to its demonstrated fidelity in hypersonic aerodynamics and aerothermodynamics. Two-dimensional steady-state reacting flowfield has been obtained by solving the Reynolds-averaged Navier-Stokes equations with the two-equation turbulence model, the shear stress transport (SST) k-ω model proposed by Menter [12]. Hydrogen-air chemical reactions are modeled using the reduced kinetic mechanism proposed by Boivin et al. which consists of 9 species and 12 reactions due to the superiority in the present range of pressure inside the scramjet combustor [13].

The computational domain is discretized by using a fully-structured mesh generated by using an open-source mesh generator Gmsh [14]. The bottom half of the combustor is calculated because the combustor is vertical symmetry. The computational mesh is displayed in Fig. 2 as an example. The combustor wall is assumed to be adiabatic while the slip wall condition is assigned for the injector slots.

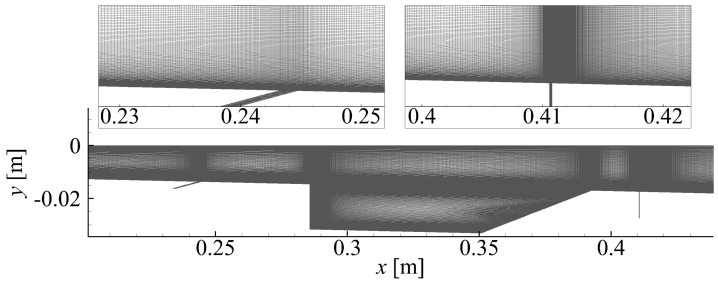

Fig. 2 Close-up view of computational mesh with nominal resolution around injectors and cavity for baseline geometry

The mesh resolution is determined by comparing three meshes with different resolutions, namely, coarse, nominal, and fine meshes. The number of cells for each mesh is summarized in Table 2. The flowfields obtained by using the meshes are compared in Fig. 3 by the streamwise distributions of static pressure and temperature on the symmetry plane. While reasonable agreement is observed for static temperature in Fig. 3 (a), substantial discrepancy is observed downstream for static temperature in Fig. 3 (b). Even with the discrepancy, a converging trend is observed among these 3 distributions, allowing for the estimation of the values without discretization error. In the present study, nominal mesh is

selected to strike the balance between accuracy and computational budget.

Table 2 Number of cells for 3 different meshes used for mesh sensitivity study

Mesh resolution	Number of cells
Coarse	129,300
Nominal	517,200
Fine	2,068,800

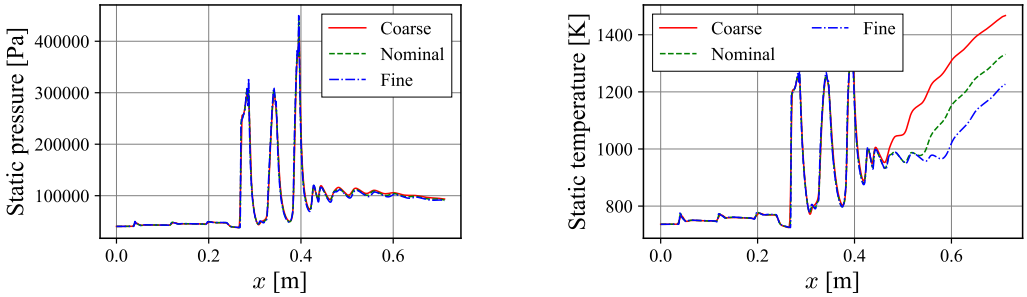

(a) Static pressure **(b)** Static temperature

Fig. 3 Comparison of streamwise distributions on symmetry plane among different meshes

2.3. Mixing and combustion performance parameters

The present study evaluates cavity-based combustor design by considering both mixing and combustion performance, which are assessed by various performance parameters. Performance of mixing and combustion is calculated at the combustor exit where the combustor height is 48.5 mm. Mixing performance is examined by considering mixing efficiency $\boldsymbol{\eta_m}$, total pressure loss $\boldsymbol{\Delta p_t}$, and streamwise force $\boldsymbol{F_x}$. Mixing efficiency quantifies the effective amount of fuel in fuel/air mixture hence the amount of the fuel that can be fairly consumed in the combustion process to the total amount of fuel injected, which is defined as:

$$\eta_{\mathrm{m}} = \frac{1}{\dot{m}_{\mathrm{H_2}}} \int_x \min\left(c_{\mathrm{H_2}}, \frac{c^s_{\mathrm{H_2}}}{c^s_{\mathrm{O_2}}} c_{\mathrm{O_2}} \right) \mathrm{d}\dot{m} \tag{1}$$

where $\dot{m}$ and c are mass flow rate and mass fraction, respectively. $c^s_{\mathrm{H_2}}$ and $c^s_{\mathrm{O_2}}$ are stoichiometric mass fractions of hydrogen and oxygen, which are 0.226 and 0.028, respectively. Total pressure loss is also considered to assess how efficiently fuel is mixed in terms of thrust generation, while a trade-off relation with mixing efficiency is recognized through preceding studies [5]. Total pressure loss is defined as:

$$\Delta p_{\mathrm{t}} = 1 - \frac{1/\dot{m} \int_x p_{\mathrm{t}} \, \mathrm{d}\dot{m}}{1/\dot{m} \int_{x=0} p_{\mathrm{t}} \, \mathrm{d}\dot{m}} \tag{2}$$

where is total pressure. Streamwise force is also considered to assess the drag force caused by aerodynamic effects, defined as:

$$F_x = \int_s (p \sin\theta + \tau \cos\theta) \, \mathrm{d}s \tag{3}$$

where s is the combustor surface area, θ is the inclination of the combustor wall, and τ is wall shear stress.

Combustion performance is assessed by using two different combustion efficiency indicators η_{c} and $\eta_{\mathrm{c,H_2O}}$, pressure ratio Π, and streamwise force F_x which is the same with Eq. (3). Combustion efficiency is evaluated by considering fuel consumption and reaction products, respectively. Combustion efficiency calculated based on fuel consumption is defined as:

$$\eta_{\mathrm{c}} = 1 - \int_x \frac{\dot{m}_{f,\mathrm{res}}}{\dot{m}_{f,\mathrm{inj}}} \mathrm{d}y \tag{4}$$

where $\dot{m}_{f,\mathrm{inj}}$ and $\dot{m}_{f,\mathrm{res}}$ are the mass flow rate of injected and remaining fuel. This value becomes 1 upstream of fuel injection and suddenly decrease at the injectors. It will then increase toward

downstream in case the combustion occurs. Another combustion efficiency η_{c,H_2O} is defined based on the reaction product hence water mass fraction, defined as:

$$\eta_{c,\,H_2O} = \frac{1}{\left(\frac{n_{H_2O}}{n_{H_2}}\right)\dot{m}_{H_2}} \int_x \rho u c_{H_2O}\,\mathrm{d}y \tag{5}$$

where $\dot{m}_{f,\mathrm{inj}}$ and $\dot{m}_{f,\mathrm{res}}$ are the mass flow rate of injected and remaining fuel. Pressure ratio is considered to measure pressure gain via combustion and indicates the capability of thrust generation through the nozzle and is defined as follows.

$$\Pi = \frac{1/\dot{m}\int_x p\,\mathrm{d}\dot{m}}{1/\dot{m}\int_{x=0} p\,\mathrm{d}\dot{m}} \tag{6}$$

2.4. Optimization

The present study conducts a design optimization study for a cavity-based scramjet combustor with the geometric representation described in Sec. 2.1. Enabling to deal with a multi-objective optimization problem, the present study employed the genetic algorithm proposed by Deb et al., which is known as NSGA-II [15]. The evolution of the population, which drives solution updates hence optimization, is repeated until the 50th generation with the 100 individuals in the population pool. The evolution consists of two phases; selection and generation of the next generation. The selection is conducted based on objective functions and constraint functions and a number of solutions are selected among the solutions in both parent and child generations. The solutions in the next generation are generated by crossover and mutation. In the case of NSGA-II, the crossover is imitated by using simulated binary crossover and the mutation is by polynomial mutation. In the present study, mutation probability is set to be 0.1 and the specified distribution index is 10 and 20 for crossover and mutation, respectively. While the solution evaluation is often conducted by employing numerical simulations, i.e., CFD, the present study employs surrogate modeling in lieu of CFD so as to drastically reduce the computational cost for solution evaluations.

Table 3 Ranges of decision variables

Decision variables	Unit	Lower limit	Upper limit
Streamwise location of cavity, l_1	m	0.015	0.050
Depth of cavity, d_c	m	0.015	0.025
Length of cavity, l_c	m	0.035	0.070
Distance between cavity and secondary injector, l_2	m	0.015	0.025
Wall inclination angle, θ_w	deg	1.000	2.300
Inclination angle of cavity backward-facing step, θ_b	deg	0.000	30.00
Inclination angle of cavity forward-facing step, θ_f	deg	15.00	45.00
Injection angle of primary injector, α_P	deg	10.00	90.00
Injection angle of secondary injector, α_S	deg	60.00	120.0
Width of primary injector, w_P	m	0.00015	0.00045
Width of secondary injector, w_S	m	0.00015	0.00045
Equivalence ratio of primary injector, Φ_P	-	0.250	0.500

The present study employs three representative performance parameters for the objective functions including combustion efficiency η_c, pressure ratio Π, and thrust F_x. The preceding study employed combustion efficiency, thrust, and total pressure loss [7,9]. Combustion efficiency is the parameters that have to be considered to evaluate how the combustion occurs. Thrust has to be considered to take the negative influence of the cavity into account and pressure ratio is considered so as to represent the capability of thrust generation through the nozzle downstream. This thus means the cases with a higher pressure ratio may result in a larger total thrust than the case with a larger thrust at the combustor

end, while the nozzle flow is not calculated in the present study. Total pressure loss is not considered in the present study because the successful heat release via supersonic combustion must result in a decrease in total pressure. All of the 12 design variables in Fig. 1 are employed as the decision variables. The ranges of decision variables are summarized in Table 3.

The optimization problem is summarized as follows.

Minimize : (1) Combustion efficiency loss, $1-\eta_c$

(2) (Inverse of) Pressure ratio, $1/\Pi$

(3) (-) Thrust, $-F_x$

2.5. Surrogate modeling

The present study employs surrogate modeling to enable design exploration with a limited computational capability. In total, 100 cases, which are generated by using Latin Hypercube Sampling [16], are evaluated via CFD and employed for surrogate modeling. While the size of the dataset is insufficient to enable accurate modeling, it is determined by the limitation of the computational cost. The range of decision variables is the same as that employed for the optimization.

Gaussian process regression (GPR) is employed for the surrogate model because it is suitable for problems with high-dimensional inputs hence the number of design variables, freeing from the curse of dimensionality. The probability distribution of the prediction from GPR can be described as follows:

$$p(y^*|\boldsymbol{x}^*, D) = \mathcal{N}(\boldsymbol{k}_*^T \boldsymbol{K}^{-1}\boldsymbol{y}, k_{**} - \boldsymbol{k}_*^T \boldsymbol{K}^{-1}\boldsymbol{k}_*) \tag{7}$$

where $\boldsymbol{K}$ is the covariance matrix that is determined by the kernel function k and the dataset D. $\boldsymbol{k}_*$ is a matrix calculated by giving $\boldsymbol{x}_*$ and the dataset D to the kernel function, and k_{**} is calculated the kernel function for $\boldsymbol{x}_*$ as the inputs. In the present study, RBF (radial basis function) kernel is employed for the kernel function, defined as follows:

$$k(\boldsymbol{x}, \boldsymbol{x}') = \theta_1 \exp\left(-\frac{|\boldsymbol{x}-\boldsymbol{x}'|^2}{\theta_2}\right) \tag{8}$$

where $\boldsymbol{x}$ and $\boldsymbol{x}'$ are the inputs, and θ_1 and θ_2 are the hyperparameters for RBF kernel. The present study employs the expectation of the prediction as the predicted value because of the stochastic behavior of GPR. Expectation of GPR prediction is described as below:

$$\mathbb{E}(y^*|\boldsymbol{x}^*, D) = \boldsymbol{k}_*^T \boldsymbol{K}^{-1}\boldsymbol{y} \tag{9}$$

3. Results

3.1. Data mining for CFD dataset

Prior to surrogate modeling and design optimization, data mining has been conducted for the dataset generated to build surrogate models in order to scrutinize the effect and sensitivity of each design parameter as well as to understand the relation among various mixing and combustion performance parameters such as mixing efficiency and total pressure loss for mixing and combustion efficiency and pressure rise for combustion. The performance parameters which are used for the objective functions are shown in Fig. 4 with respect to wall inclination angle θ_w and equivalence ratio of P injector Φ_P. Wall inclination angle θ_w has significant influence on all performance parameters. It is important to clarify the physical rationale behind the large sensitivity of θ_w, which varies both the expansion angle and length of the combustor wall. The expansion angle may influence combustion characteristics by varying static pressure and static temperature, whereas the total length of the combustor has significant impact on the flow residence time that directly influences the combustion efficiency.

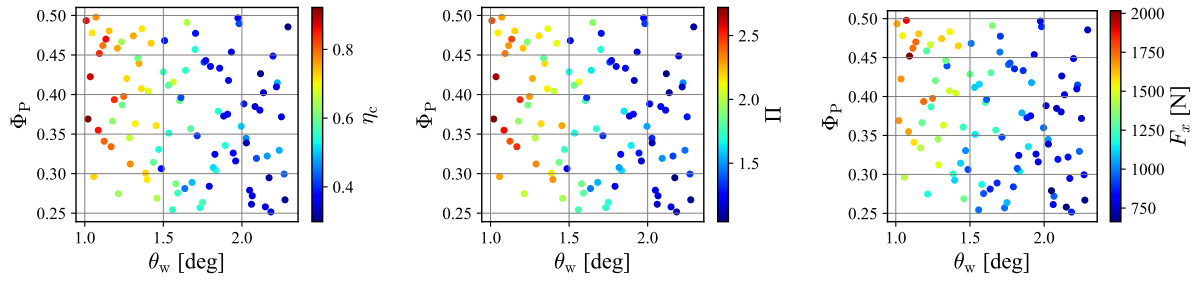

(a) Combustion efficiency **(b)** Pressure ratio **(c)** Thrust

Fig. 4 Performance distributions against wall inclination angle and equivalence ratio of Primary injector

The flowfields of the 5 cases with the largest and smallest θ_w have been selected, respectively to investigate the physical ground of the effect of θ_w. Combustion efficiency is compared between the cases with small θ_w and large θ_w in Fig. 5. Here, combustion efficiency that is defined by the mass flow rate of H_2O (Eq. (7)) is considered so as to investigate the distribution of the reaction product. In the case with small θ_w (Fig. 5 (a)), combustion efficiency becomes higher than those with large θ_w (Fig. 5 (b)) at the same location, indicating that the larger wall inclination degrades combustion efficiency due to the decrease of static pressure caused by the expansion of the flow channel. Therefore, the superiority of small θ_w is brought by the influence of higher static pressure than the cases with large θ_w. The wall pressure distributions in frozen flow are compared in Fig. 6. There exists a tendency that smaller θ_w results in higher wall pressure and this verifies that the pressure decrease affects the

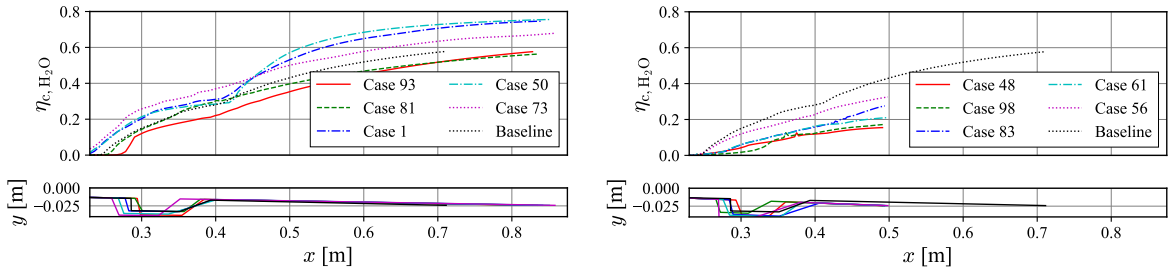

(a) Cases with 5 smallest θ_w **(b)** Cases with 5 largest θ_w

Fig. 5 Combustion efficiency distributions for cases with 5 smallest and largest wall inclination angle combustion.

Extracting the features of the combustor design that achieves favorable performance, two cases with the best performance in terms of combustion efficiency and thrust are selected and investigated by comparing them with the baseline geometry. The performance of the selected and baseline geometries is summarized in Table 4. The case with the largest compression ratio has become the same as the case with the largest combustion efficiency.

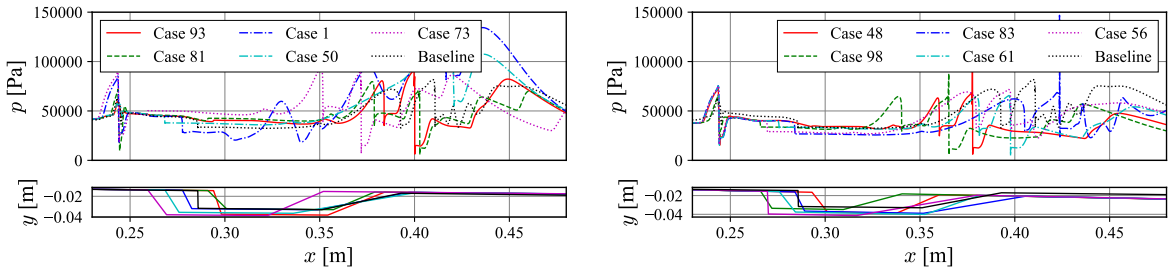

(a) Cases with 5 smallest θ_w **(b)** Cases with 5 largest θ_w

Fig. 6 Wall pressure distributions in the vicinity of cavity for cases with 5 smallest and largest wall inclination angle

Table 4 Comparison of combustor performance for selected and baseline geometries

Case	Reason	Frozen			Reacting		
		η_m	Δp_t	F_x	η_c	Π	F_x
Case 50	Largest η_c and Π	0.6773	0.6625	-308 N	0.9220	2.720	1679 N
Case 78	Largest F_x	0.4555	0.5278	91 N	0.8403	2.358	2016 N
Baseline	-	0.4868	0.5105	-19 N	0.7337	2.267	1380 N

It is interesting to note that the case with the largest F_x is characterized by a smaller mixing efficiency yet larger thrust. Streamwise variations of thrust force are compared in Fig. 7. The thrust increase around x=0.025 m is caused by the backward-facing step of the cavity and the thrust decrease is caused by the forward-facing step. In the case with the largest thrust, the thrust decrease caused by the forward-facing step is the smallest among 3 geometries, indicating the drag caused by the cavity. While case 50 has the largest combustion efficiency, the thrust force is not the largest due to the large cavity drag. Therefore, it is important to design cavities by considering the positive effect due to the efficient and stable combustion and the negative effect that is the aerodynamic drag simultaneously, indicating the necessity of performing multi-objective design optimization of a cavity and injectors in scramjet combustors.

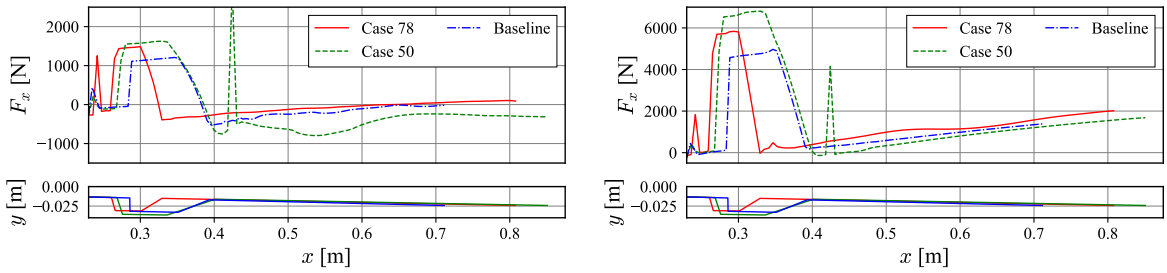

(a) Frozen **(b)** Reacting

Fig. 7 Comparison of streamwise variations of thrust

The design factors for higher combustion efficiency are discussed here. Except for the effect of wall inclination angle, which is discussed above, the cavity design and injection conditions are the candidates of influential design factors. The cavity and injector design of Case 50 is expected to play an important role in enhancing fuel mixing and combustion. Fig. 8 displays streamwise variations of mixing efficiency and fuel mass fraction distributions in the vicinity of cavities for Cases 78 and 50. It has been seen in Fig. 8 (a) that the mixing efficiency increases from the location where the forward-facing step starts, indicating that the forward-facing step of the cavity plays an important role in mixing enhancement. Distributions of effective hydrogen mass fraction inside the cavity (Fig. 8 (b)) also indicate that fuel/air mixing inside the cavity is more enhanced in Case 50 than in Case 78. In addition, Case 50 is characterized by the large increase in mixing efficiency at the Secondary injector (Fig. 8 (a)). Flow structures in the vicinity of the cavity and Secondary injector are compared between Cases 78 and 50 in Fig. 9. While the pressure distribution of Case 78 has a pressure decrease between the forward-facing step and Secondary injector, Case 50 is characterized by the merger of the pressure rise caused by the forward-facing step and the pressure rise caused by the Secondary injector. Mach number distributions are compared in Fig. 9 (b) and the subsonic region is represented by the white regions. In Case 50, the subsonic regions between the cavity and the Secondary injector are merged and a small recirculation zone is caused upstream of the injector. This allows for further penetration of the mixture through the cavity, resulting in a higher mixing efficiency. This thus indicates that there may exist a favorable combination of the cavity and Secondary injector, suggesting the design optimization of a cavity-based combustor.

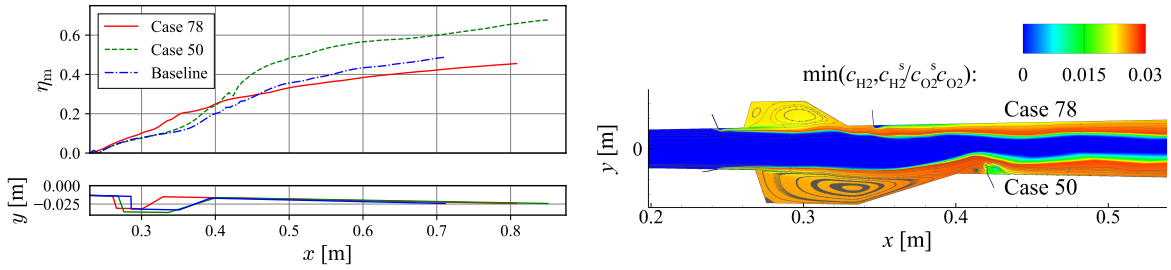

(a) Mixing efficiency **(b)** Effective fuel mass fraction

Fig. 8 Influence of cavity and injector design on mixing performance

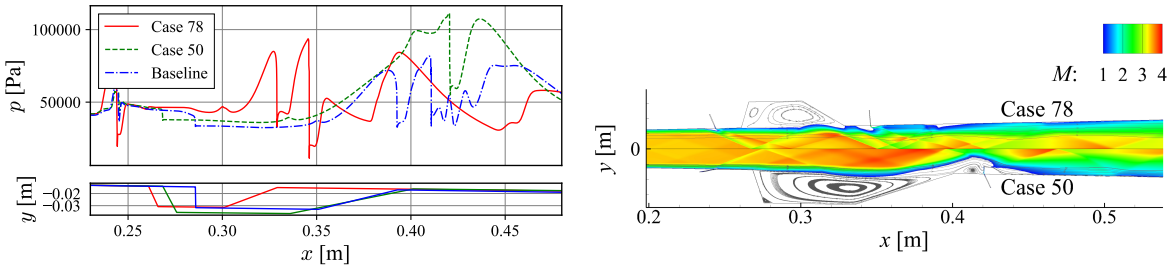

(a) Wall pressure distributions **(b)** Mach number distributions and subsonic regions

Fig. 9 Comparison of flow structures in the vicinity of cavity and secondary injector

Combustion characteristics are compared between Cases 78 and 50. Case 50 is characterized by a larger density of water downstream of the Secondary injector, while Case 78 is characterized by a higher density of water inside the cavity, as seen in Fig. 10 (a). This difference can be explained by the difference in OH distributions. While Case 78 has almost completed the reactions inside the cavity, the cavity of Case 50 plays a role in producing OH radicals. This helps to sustain combustion downstream, resulting in higher combustion efficiency. Further investigation is required to identify the design features that contribute to efficient combustion and thrust generation.

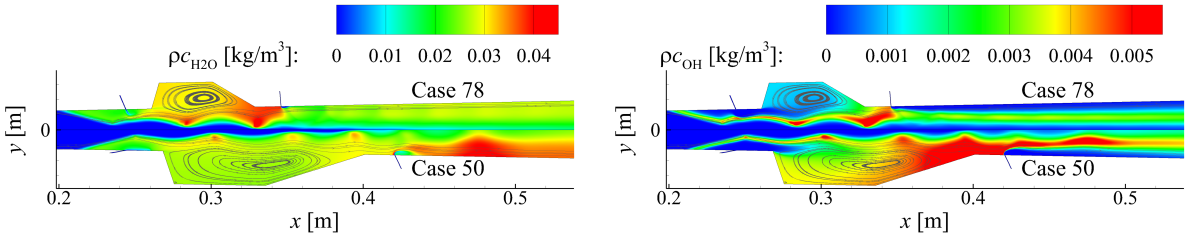

(a) Hydrogen density distributions **(b)** OH density distributions

Fig. 10 Comparison of species density distributions in the vicinity of cavity

3.2. Model-based optimization

Model-based multi-objective design optimization has been conducted to investigate key design features to maximize thrust and combustion efficiency. The CFD simulations for solution evaluations are replaced by a surrogate model using Gaussian process regression (GPR). The prediction accuracy for training data has been shown in Fig. 11. While the accuracy is relatively low, the GPR models capture the trends of performance parameters. These models are thus employed for the optimization.

The optimization results are displayed in the objective function space in Fig. 12, focusing on the Pareto optimal front. Trade-off relations have been observed between thrust and pressure ratio as well as thrust and combustion efficiency, while combustion efficiency and pressure ratio do not conflict with each other. This tendency is consistent with the observation in the dataset that the maximum combustion efficiency and maximum pressure ratio are achieved simultaneously. The trade-off relation between combustion efficiency and thrust can be explained by considering the differences in the design of Cases 78 and 50, which are characterized by the largest thrust and combustion efficiency, respectively. Higher combustion efficiency has been achieved due to the successful mixing and OH

production in the cavity and the secondary injection toward upstream, but both of these characteristics of the design are the factors to decrease thrust: The larger cavity tends to increase the drag, and the injection toward upstream gives the negative momentum to the mainstream. Further detailed investigation is required to elucidate the influences of decision variables on combustor performance, and the accuracy of the prediction model has to be further enhanced with a small increase in the computational cost for CFD simulations.

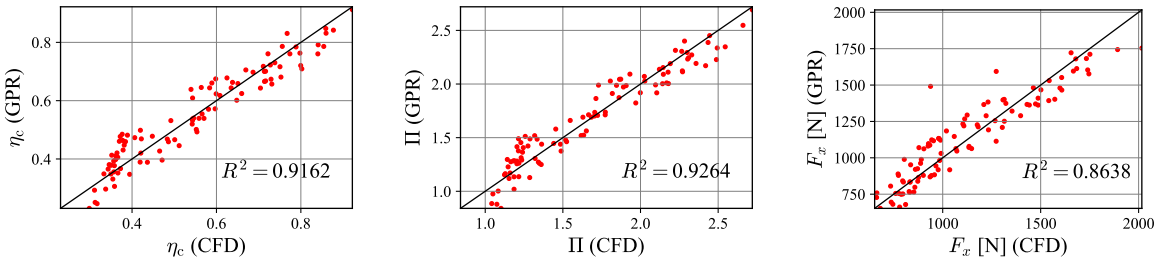

(a) Combustion efficiency **(b)** Pressure ratio **(c)** Streamwise force

Fig. 11 Comparison between prediction (GPR) and actual evaluation (CFD) for training data

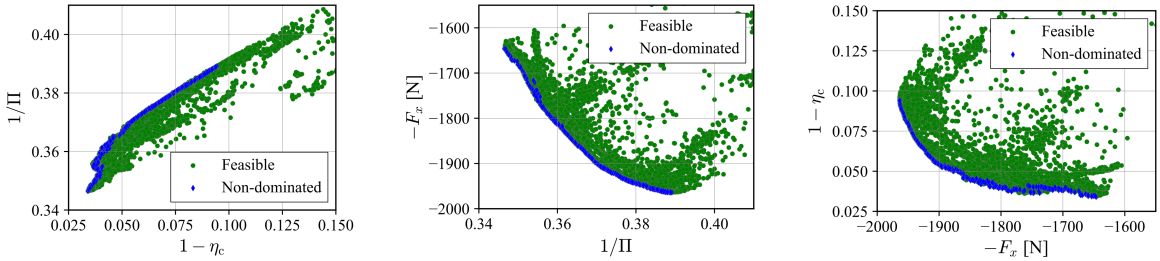

(a) $1-\eta_c$ vs $1/\Pi$ **(b)** $1/\Pi$ vs $-F_x$ **(c)** $-F_x$ vs $1-\eta_c$

Fig. 12 Solution distributions in objective function space and Pareto optimal front

3.3. Discussions on data-efficient surrogates

While conventional surrogate models enable accurate prediction based on a dataset large enough, it is a hard task for reacting flow simulations to prepare a dataset with a substantial computational cost. Thus, it is important to reduce the number of data required as well as to utilize a given dataset efficiently. A potential approach is the improvement of the sampling strategy. Several approaches for the design of experiments are employed for efficient initial sampling [17]. Additional sampling strategies based on Kriging and radial basis functions are also applicable approaches to achieve a specified accuracy with a smaller number of training data [18]. Another way for data-efficient surrogate modeling is the prediction based on the simplified problem, *e.g.*, prediction of the 3D flowfields by employing the 2D flowfields which are the simplified problems of the 3D flowfields as the inputs. This type of predictive framework is reported by Yu and Hesthaven for flowfield prediction [19].

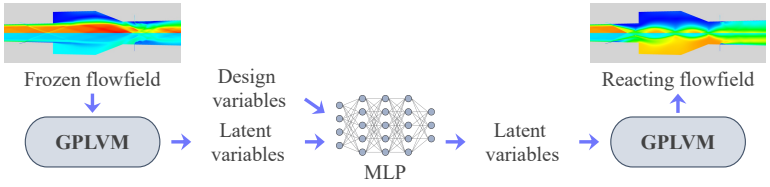

Fig. 13 Part of flowfield prediction framework developed in the present study

The present study developed a predictive framework that predicts reacting flowfields which require substantial computational cost to be obtained based on chemically frozen flowfields which require much a smaller computational cost than reacting flowfields. The predictive framework is designed based on the preceding study by Yu and Hesthaven [19] and a ROM-based predictive framework [20]. A part of the predictive framework developed in the present study is displayed in Fig. 13. Since it is difficult to obtain the latent variables of the frozen flowfield for the geometries that are not used for the development of GPLVM (Gaussian process latent variable modeling), which is a reduced-order modeling

technique, the present structure in Fig. 13 is defective in construction to achieve the prediction of reacting flowfields from scratch for unseen geometries. The results of flowfield reconstruction for the data used to build GPLVM are displayed in Figs. 14 and 15. While there exist several regions with unignorable large prediction errors, the flow structures are reasonably reconstructed even with the smaller number of training data. Further development is required so as to enable predictive modeling with a smaller number of training data.

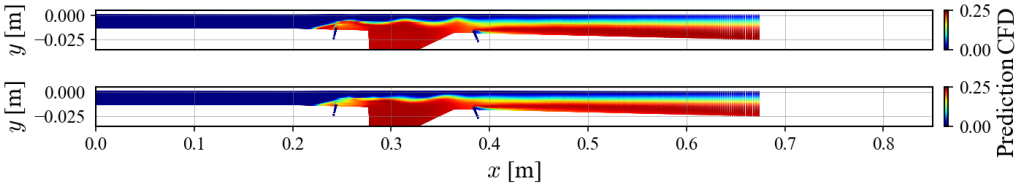

Fig. 14 Comparison of H2O mass fraction between CFD and prediction

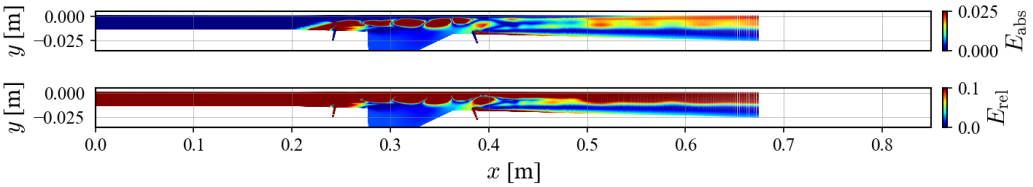

Fig. 15 Distributions of prediction errors in the form of absolute and relative errors

4. Conclusions

The present study conducted design exploration for cavity-based scramjet combustors based on a relatively small CFD dataset to extract key design factors and gain physical insights into rationales behind the favorable design of cavity-based combustors. The CFD dataset comprising 100 geometries has been scrutinized to understand the influence of design parameters on mixing and combustion performance from a global point of view. A model-based optimization study has then been conducted to explore the optimum combination of design features in the design space.

The data mining of the CFD dataset has revealed a significant influence of wall inclination angle on performance parameters. The effects of the remaining design parameters have been discussed by selecting two cases with the largest thrust and the highest combustion efficiency and pressure ratio, respectively. The case with the largest thrust is characterized by the smaller cavity, which is one of the largest sources of drag force, yet the combustion efficiency is adequate. On the other hand, the case with the highest combustion efficiency is characterized by a large cavity that successfully produces OH radicals downstream, sustaining supersonic combustion downstream of the secondary injector. A model-based design optimization has then been conducted to gain physical insights into the cavity-based scramjet combustor design that maximizes combustion efficiency, pressure ratio, and thrust. Trade-off relations have been observed between combustion efficiency and thrust as well as between pressure ratio and thrust.

Furthermore, a flowfield-prediction framework with small datasets of reacting flowfields has been discussed. While the prediction accuracy is yet to be improved to be useful for design exploration, future efforts will warrant a new effective methodology to develop accurate surrogates with a relatively small dataset.

Acknowledgement

The authors acknowledge the support provided by the Japan Society for the Promotion of Science (JSPS) through the Grant-in-Aid for JSPS Fellows Grant Number 22J20613 (22KJ2460) and the KAKENHI Grant number 17K20144 as well as the Japan Science and Technology Agency through the JST SPRING Grant Number JPMJSP2136. The authors would like to thank Dr. Masatoshi Kodera and Dr. Masaaki Fukui for technical assistance with CFD simulations and Ms. Miyu Shimmoto and Mr. Tomoaki Nara for fruitful discussion on combustion and combustor design.

References

1. Smart, M.K., Hass, N.E., and Paull, A.: Flight Data Analysis of the HyShot 2 Scramjet Flight Experiment. AIAA J. 44, 2366-2375 (2006)
2. McClinton, C.R., Rausch, V.L., Nguyen, L.T., and Sitz, J.R.: Preliminary X-43 flight test results. Acta Astronaut. 57, 266-276 (2005)
3. Hank, J.M., Murphy, J.S., and Mutzman, R.C.: The X-51A Scramjet Engine flight demonstration program. AIAA Paper 2008-2540 (2008)
4. Fujio, C. and Ogawa, H.: Physical insights into multi-point global optimum design of scramjet intakes for ascent flight. Acta Astronaut. 194, 59-75 (2022)
5. Huang, W., Yang, J., and Yan, L.: Multi-objective design optimization of the transverse gaseous jet in supersonic flows. Acta Astronaut. 93, 13-22 (2014)
6. Ogawa, H. and Boyce, R.R.: Nozzle Design Optimization for Axisymmetric Scramjets by Using Surrogate-Assisted Evolutionary Algorithms. J. Propuls. Power 28, 1324-1338 (2013)
7. Kumar, S., Das, S., and Sheelam, S.: Application of CFD and the Kriging method for optimizing the performance of a generic scramjet combustor. Acta Astronaut. 101, 111-119 (2014)
8. Gerlinger, P., Nold, K., and Aigner, M.: Influence of reaction mechanisms, grid spacing, and inflow conditions on the numerical simulation of lifted supersonic flames. Int. J. Numer. Meth. Fluids 62, 1357–1380 (2010)
9. Ogawa, H., Boyce, R.R., Isaacs, A., and Ray, T.: Multi-Objective Design Optimisation of Inlet and Combustor for Axisymmetric Scramjets. The Open Thermodynamics Journal 4, 86-91 (2010)
10. Jackson, K.R., Gruber, M.R., and Barhorst, T.F. :The HIFiRE Flight 2 Experiment: An Overview and Status Update. AIAA Paper 2009-5029 (2009)
11. CFD++, Software Package, Ver. 21.1, Metacomp Technologies, Agoura Hills, CA, (2020)
12. Menter, F.R.: Two-Equation Eddy-Viscosity Turbulence Models for Engineering Applications. AIAA J. 32, 1598-1605 (1994)
13. Boivin, P., Jiménez, C., Sánchez, A. L., and Williams, F. A.: An explicit reduced mechanism for H2-air combustion. Proc. Combust. Inst. 33, 17-523 (2011)
14. Geuzaine, C.: Gmsh : A 3-D finite element mesh generator with built-in pre- and post-processing facilities. Int. J. Numer. Meth. Engng. 79, 1309-1331 (2009)
15. Deb, K., Pratap, A., Agarwal, S., and Meyarivan, T.: A Fast and Elitist Multiobjective Genetic Algorithm :NSGA-II. IEEE Trans. Evol. Comput. 6, 182-197 (2002)
16. Stein, M.: Large sample properties of simulations using latin hypercube sampling. Technometrics, 29, 143-151 (1987)
17. Yondo, R., Andrés, E., and Valero, E.: A review on design of experiments and surrogate models in aircraft real-time and many-query aerodynamic analyses, Prog. Aerosp. Sci., 96, 23-61 (2018)
18. Mackman, T.J., Allen, C.B., Ghoreyshi, M., and Badcock, K.J.: Comparison of Adaptive Sampling Methods for Generation of Surrogate Aerodynamic Models, AIAA J. 51, 797-808 (2013)
19. Yu, J. and Hesthaven, J.S.,: Flowfield Reconstruction Method Using Artificial Neural Network, AIAA J. 57, 482-498 (2019)
20. Fujio, C., Akiyama, K., and Ogawa, H.: Fast and reliable prediction of scramjet flowfields via Gaussian process latent variable model and deep learning, Phys. Fluids, 35 (2023)